# Statistical measurements of quantum emitters coupled to Anderson-localized modes in disordered photonic-crystal waveguides

**Alisa Javadi,[1,*] Sebastian Maibom,[1] Luca Sapienza,[1,2] Henri Thyrrestrup,[1,3] Pedro D. García,[1] and Peter Lodahl[1,4]**

[1] *Niels Bohr Institute, University of Copenhagen, Blegdamsvej 17, DK-2100 Copenhagen, Denmark*

[2] *Current address: School of Physics & Astronomy, University of Southampton, Southampton SO17 1BJ, UK*

[3] *Current address: MESA+ Institute for Nanotechnology, University of Twente, 7500 AE Enschede, The Netherlands*

[4] *lodahl@nbi.ku.dk*

[*] *javadi@nbi.ku.dk*

*www.quantum-photonics.dk*

**Abstract:** We present a statistical study of the Purcell enhancement of the light emission from quantum dots coupled to Anderson-localized cavities formed in disordered photonic-crystal waveguides. We measure the time-resolved light emission from both single quantum emitters coupled to Anderson-localized cavities and directly from the cavities that are fed by multiple quantum dots. Strongly inhibited and enhanced decay rates are observed relative to the rate of spontaneous emission in a homogeneous medium. From a statistical analysis, we report an average Purcell factor of $4.5\pm0.4$ without applying any spectral tuning. By spectrally tuning individual quantum dots into resonance with Anderson-localized modes, a maximum Purcell factor of $23.8\pm1.5$ is recorded, which is at the onset of the strong-coupling regime. Our data quantify the potential of Anderson-localized cavities for controlling and enhancing the light-matter interaction strength in a photonic-crystal waveguide, which is of relevance for cavity quantum-electrodynamics experiments, efficient energy harvesting and random lasing.



**OCIS codes:** (270.5580) Quantum electrodynamics; (290.4210) Multiple scattering.

## References and links

1. L. Novotny and B. Hecht, *Principles of Nano-Optics* (Cambridge University, 2006).
2. E. M. Purcell, "Spontaneous emission probabilities at radio frequencies," Phys. Rev. **69**, 681 (1946).
3. P. Lodahl, A. F. van Driel, I. S. Nikolaev, A. Irman, K. Overgaag, D. Vanmaekelbergh, and W. L. Vos, "Controlling the dynamics of spontaneous emission from quantum dots by photonic crystals," Nature **430**, 654-657 (2004).
4. D. Englund, D. Fattal, E. Waks, G. Solomon, B. Zhang, T. Nakaoka, Y. Arakawa, Y. Yamamoto, and J. Vučković, "Controlling the spontaneous emission rate of single quantum dots in a two-dimensional photonic crystal," Phys. Rev. Lett. **95**, 013904 (2005).

#223550 - $15.00 USD Received 22 Sep 2014; revised 13 Nov 2014; accepted 14 Nov 2014; published 5 Dec 2014

5. Q. Wang, S. Stobbe, and P. Lodahl, "Mapping the local density of optical states of a photonic crystal with single quantum dots," Phys. Rev. Lett. **107**, 167404 (2011).
6. T. Yoshie, A. Scherer, J. Hendrickson, G. Khitrova, H. M. Gibbs, G. Rupper, C. Ell, O. B. Shchekin, and D. G. Deppe, "Vacuum Rabi splitting with a single quantum dot in a photonic crystal nanocavity," Nature **432**, 200–203 (2004).
7. J. D. D. Joannopoulos, S. G. G. Johnson, J. N. N. Winn, and R. D. D. Meade, *Photonic crystals: Molding the Flow of Light* (Princeton University, 2008).
8. H. Thyrrestrup, L. Sapienza, and P. Lodahl, "Extraction of the $\beta$-factor for single quantum dots coupled to a photonic crystal waveguide," Appl. Phys. Lett. **96**, 231106 (2010).
9. T. Baba, "Slow light in photonic crystals," Nature Photonics **2**, 465–473 (2008).
10. M. Eichenfield, J. Chan, R. M. Camacho, K. J. Vahala, and O. Painter, "Optomechanical crystals ," Nature **462**, 78–82 (2009).
11. T. Lund-Hansen, S. Stobbe, B. Julsgaard, H. Thyrrestrup, T. Sünner, M. Kamp, A. Forchel, and P. Lodahl, "Experimental realization of highly efficient broadband coupling of single quantum dots to a photonic crystal waveguide," Phys. Rev. Lett. **101**, 113903 (2008).
12. M. Arcari, I. Söllner, A. Javadi, S. Lindskov Hansen, S. Mahmoodian, J. Liu, H. Thyrrestrup, E. H. Lee, J. D. Song, S. Stobbe, and P. Lodahl, "Near-unity coupling efficiency of a quantum emitter to a photonic crystal waveguide," Phys. Rev. Lett. **113**, 093603 (2014).
13. S. Hughes, L. Ramunno, J. F. Young, and J. E. Sipe, "Extrinsic optical scattering loss in photonic crystal waveguides: Role of fabrication disorder and photon group velocity," Phys. Rev. Lett. **94**, 033903 (2005).
14. D. Gerace and L. C. Andreani, "Disorder-induced losses in photonic crystal waveguides with line defects,," Opt. Lett. **29**, 1897–1899 (2004).
15. S. Mazoyer, J. P. Hugonin, and P. Lalanne, "Disorder-induced multiple scattering in photonic-crystal waveguides," Phys. Rev. Lett. **103**, 063903 (2009).
16. E. Kuramochi, M. Notomi, S. Hughes, A. Shinya, T. Watanabe, and L. Ramunno, "Disorder-induced scattering loss of line-defect waveguides in photonic crystal slabs," Phys. Rev. B **72**, 161318(R) (2005).
17. S. John, "Strong localization of photons in certain disordered dielectric superlattices," Phys. Rev. Lett. **58**, 2486 (1987).
18. P. W. Anderson, "Absence of diffusion in certain random lattices," Phys. Rev. **109**, 1492 (1958).
19. V. Savona, "Electromagnetic modes of a disordered photonic crystal," Phys. Rev. B **83**, 085301 (2011).
20. S. R. Huisman, G. Ctistis, S. Stobbe, A. P. Mosk, J. L. Herek, A. Lagendijk, P. Lodahl, W. L. Vos, and P. W. H. Pinkse, "Measurement of a band-edge tail in the density of states of a photonic-crystal waveguide," Phys. Rev. B **86**, 155154 (2012).
21. P. Sheng, *Introduction to Wave Scattering, Localization, and Mesoscopic Phenomena* (Academic Press, 1995).
22. J. Topolancik, B. Ilic, and F. Vollmer, "Experimental observation of strong photon localization in disordered photonic crystal waveguides," Phys. Rev. Lett. **99**, 253901 (2007).
23. J. Topolancik, F. Vollmer, R. Ilic, and M. Crescimanno, "Out-of-plane scattering from vertically asymmetric photonic crystal slab waveguides with in-plane disorder," Opt. Express **17**, 12470–12480 (2009).
24. Y. Akahane, T.i Asano, B. Song, and S. Noda, "High-Q photonic nanocavity in a two-dimensional photonic crystal," Nature **425**, 944–947 (2003).
25. L. Sapienza, H. Thyrrestrup, S. Stobbe, P. D. García, S. Smolka, and P. Lodahl, "Cavity Quantum electrodynamics with Anderson-localized modes," Science **327**, 1352–1355 (2010).
26. K. Vynck, M. Burresi, F. Riboli, and D. S. Wiersma, "Photon management in two-dimensional disordered media," Nature Mater. **11**, 1017–1022 (2012).
27. H. E. Türeci, L. Ge, S. Rotter, and A. D. Stone, "Strong interactions in multimode random lasers," Science **320**, 643–646 (2008).
28. J. Liu, P. D. García, S. Ek, N. Gregersen, T. Suhr, M. Schubert, J. Mørk, S. Stobbe, and P. Lodahl, "Random nanolasing in the Anderson localized regime," Nature Mat. **9**, 285–289 (2014).
29. H. Thyrrestrup, S. Smolka, L. Sapienza, and P. Lodahl, "Statistical theory of a quantum emitter strongly coupled to Anderson-localized modes," Phys. Rev. Lett. **108**, 113901 (2012).
30. S. Smolka, H. Thyrrestrup, L. Sapienza, T. B. Lehmann, K. R. Rix, L. S. Froufe-Pérez, P. D. García, and P. Lodahl, " Probing the statistical properties of Anderson localization with quantum emitters," New J. Phys. **13**, 063044 (2011).
31. M. Patterson, and S. Hughes, "Interplay between disorder-induced scattering and local field effects in photonic crystal waveguides," Phys. Rev. B **81**, 245321 (2010).
32. A. Kiraz, P. Michler, C. Becher, B. Gayral, A. Imamoğlu, L. Zhang, E. Hu, W. V. Schoenfeld, and P. M. Petroff, "Cavity-quantum electrodynamics using a single InAs quantum dot in a microdisk structure ," Appl. Phys. Lett. **78**, 3932 (2001).
33. J. Gao, S. Combrie, B. Liang, P. Schmitteckert, G. Lehoucq, S. Xavier, X. Xu, K. Busch, D. Huffaker, A. De Rossi, and C. W. Wong, "Strongly coupled slow-light polaritons in one-dimensional disordered localized states," Sci. Rep. **3**, 1994 (2013).

#223550 - $15.00 USD Received 22 Sep 2014; revised 13 Nov 2014; accepted 14 Nov 2014; published 5 Dec 2014

## 1. Introduction

The local environment of a quantum emitter determines its spectral and spatial emission properties. Within the dipole approximation, the emission dynamics of an emitter is directly determined by the local density of optical states (LDOS) [1], which accounts for the density of vacuum fluctuation at the position of the emitter. By tailoring the LDOS it is possible to increase (decrease) the coupling strength between the quantum emitter and its environment and enhance (inhibit) the emitter spontaneous-emission rate through the Purcell effect [2]. For a sufficiently large coupling strength, a single emitter and a single electromagnetic mode can even become entangled which is referred to as strong coupling. Among the different approaches for tailoring the LDOS by nanoengineering, photonic crystals (PhC) have so far been the most successful. Controlled spontaneous emission [3, 4] with modifications of the emission rate approaching two orders of magnitude [5] have been demonstrated together with strong coupling between a single quantum dot and a photon in a photonic-crystal cavity [6]. PhCs are dielectric structures where a periodic variation of the refractive index leads to the formation of a frequency range, the photonic bandgap, where electromagnetic wave propagation is strongly suppressed [7]. One possible implementation of a two dimensional PhC is obtained by etching a hexagonal lattice of holes in a membrane of a high refractive index material. In such a PhC, a photonic-crystal waveguide (PhCW) is formed by leaving out a row of holes, see Fig. 1(a). In that case, the light is tightly confined and effectively guided along the missing row of holes due to the presence of an in-plane bandgap in the PhC and by total internal reflection within the membrane. Two different (longitudinal) waveguide modes are found in the bandgap, cf. the dispersion diagram of Fig. 1(b) and the mode profiles in Figs. 1(c) and 1(d). At the edges of a PhC bandgap and close to the cut-off of the waveguide modes, the LDOS is strongly enhanced diverging in the case of a perfect crystal. This effect is called the Van-Hove singularity and implies an ideally vanishing waveguide mode group velocity thus forming a standing wave. In real structures, fabrication imperfections smooth this singularity, but a strongly enhanced LDOS still prevails near the cutoff of the waveguide mode [8]. This ability to enhance the LDOS makes PhCs and PhCWs very useful for slowing down light [9], optomechanical experiments [10] and deterministic photon-emitter interfaces [11, 12] for quantum-information applications.

The presence of disorder in a PhCW, ultimately due to the limited precision of fabrication processes, breaks the discrete translational symmetry. Disorder degrades the performance of the PhCWs and increases the propagation loss in the waveguide [13–16] by inducing random multiple scattering of light and creating one-dimensional Anderson-localized modes [17, 18]. The Anderson-localized modes approximately inherit the polarization properties of the propagating modes in the waveguide, as seen in Fig. 1(c) and 1(d). Due to their random nature, a statistical analysis is required to extract the spectral and spatial properties of these modes. They appear around and below the cut-off frequency of the waveguide mode or at the bandedge forming a so-called Lifshitz tail [19, 20], as marked in Fig. 1(b) by the shadowed regions for the waveguide modes. After ensemble averaging over all configurations of disorder, the electric field from an embedded emitter will decay exponentially in space with a characteristic length called the localization length ($\xi$) [21]. A finite-element calculation of the $E_y$ components of two different Anderson-localized modes is shown in Figs. 1(c) and 1(d) that is compared to the Bloch modes of the ideal periodic structure. Remarkably, such random cavities in a PhCW have been found to have quality (Q) factors and mode volumes that are comparable to state-of-the-art engineered cavities [22–24], both in silicon-based structures [22] and in optically active materials such as GaAs [25], with the benefit of having less stringent requirements on sample fabrication precision. Disorder-induced cavities have attracted significant attention and have been proposed for light harvesting application [26], used in cavity quantum electrodynamic (QED) experiments [25] and for random lasing [27, 28].

#223550 - $15.00 USD Received 22 Sep 2014; revised 13 Nov 2014; accepted 14 Nov 2014; published 5 Dec 2014

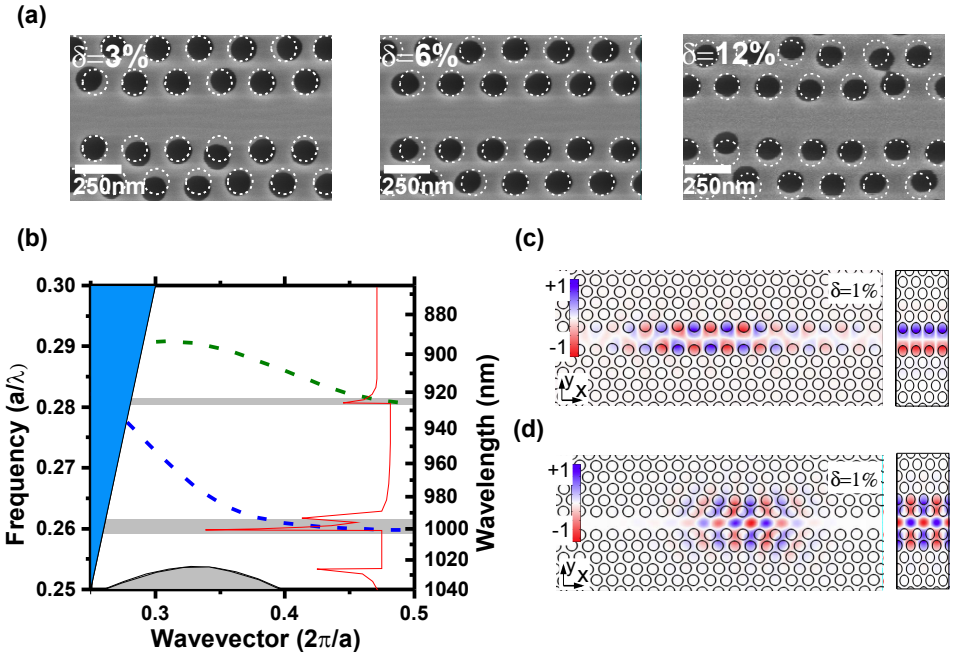


**Fig.** 1. **Anderson localization in photonic-crystal waveguides.** (a) Scanning-electron micrographs of photonic-crystal waveguides with different amounts of intentional disorder in the hole position. Dashed circles indicate the positions of the holes in a perfectly periodic structure. (b) Dispersion relation for an ideal photonic-crystal waveguide showing the fundamental (dashed blue line) and high-energy (green) guided modes from a full 3D simulation of a photonic-crystal membrane structure. The blue area corresponds to the light cone where the radiation is not bound to membrane. The band gap of the photonic crystal extends from $a/\lambda = 0.255$ to the top of the figure. The shadowed area near the cutoff of the guided modes indicate the spectral range where Anderson-localized modes appear. The red curve is a sketch of the local density of optical states of a disordered structure. (c) and (d) Illustration of Anderson-localized modes obtained from 2D finite-element calculation of the $E_y$ component of the electric field in a disordered perturbed PhCW with $\sigma = 1\%$ introduced disorder in the hole positions (left) and along an unperturbed PhCW (right) corresponding to the high-energy ($\lambda = 850$ nm) (c) and fundamental ($\lambda = 930$ nm) (d) guided modes shown in (b).

The complex nature of multiple scattering of light in disordered systems requires a statistical approach that accounts for the statistical distribution of the relevant physical parameters describing the system. The probability of entanglement between a single quantum dot and a photon in an Anderson-localized mode in a disordered PhCW has been investigated [29], where a probability of 1% was found for parameters corresponding to present experiments. In addition, from the statistical distribution of Purcell factors the probability to observe largely enhanced decay rates was assessed. The main goal of the present article is to give the first experimental study of the statistics of the decay rate of emitters embedded in disordered PhCWs. In this paper, we present statistical measurements of the decay dynamics of both for the case where the cavities are probed directly and for the case that single quantum dots are tuned into resonance with Anderson-localized modes. The data sets provide two alternative ways of extracting experimentally Purcell factor statistics. In the first presented data set we measure the decay

#223550 - $15.00 USD Received 22 Sep 2014; revised 13 Nov 2014; accepted 14 Nov 2014; published 5 Dec 2014

dynamics of the Anderson-localized modes and extract the fastest rate of the multi-exponential decay curves. This procedure records the rate of the quantum dot that is best coupled to this particular Anderson-localized mode while the detuning between the emitter and the cavity is not optimized. For the second data set, we tune a single quantum dot through resonance of an Anderson-localized mode. This uncovers the full potential of the Anderson-localized modes but at the expense that the measurements are time consuming thereby limiting the amount of statistical data that can be collected. From our measurements, we evaluate the light-matter interaction strength and compare the experimental data to the theoretically predicted distributions illustrating that the best observed cavities are at the onset of the strong-coupling regime.

## 2. Experimental methods

The samples studied are 150 nm thick GaAs membranes with an embedded layer of self-assembled InAs quantum dots in the center with a density of 80 $\mu m^{-2}$ that emit light in the 890 nm - 1000 nm wavelength range. A set of 100 $\mu$m long PhCWs with a hexagonal lattice of holes and varying lattice constant ($a$) and hole radius ($r$) are etched in the membrane. All waveguides are at least 10 times longer than the measured localization length [30], meaning that Anderson-localized modes are formed near the cut-off of the waveguide mode. Various types of disorder likely contribute to the intrinsic disorder, including uncertainties in the positions and radii of the holes as well as surface roughness. Modeling imperfections in PhCWs have been successfully achieved for the cases of hole radii variations [15] and fluctuations in the hole positions [19, 31]. For the present work, apart from intrinsic fabrication imperfections in shape, size, and position of the holes, additional engineered disorder is introduced in the sample by randomly varying the position of the three rows of holes on each side of the waveguide according to a normal distribution with a mean value of zero and a variance of $\sigma \times a$ where $\sigma$ is varied from 0% to 12% (cf. Fig. 1(a)). Figure 2(a) schematically represents two quantum dots at two different positions showing the two potential dipole orientations with respect to the $E_y$ field component of an Anderson-localized mode in a PhCW. For carrying out the optical measurements, the sample is placed in a liquid Helium flow cryostat and cooled down to 10 K, see Fig. 2(b). A pulsed Ti:Sapphire laser with 5 pico-second pulse width emitting at 800 nm is focused on the sample through a microscope objective with NA = 0.55 from the top to a spot size of about 1.4 $\mu m^2$, and the emission from the quantum dots is collected through the same microscope objective. The cryostat is mounted on translational stages to control the excitation and collection positioning with an accuracy of 100 nm. The emission is polarization filtered with a half-wave plate and a polarizing beam-splitter, coupled to a polarization maintaining single mode fiber for spatial filtering, and sent to a monochromator with spectral resolution of 50 pm. The filtered light is finally detected with a CCD for spectral measurements or with an avalanche photo diode (APD) for time-resolved measurements.

Time-resolved measurements are performed using two different approaches. In the first one, a set of waveguides with lattice constant a = 240 nm, hole radius r = 74 nm, and different disorder degrees (0-5% and 9%) are investigated, where the cut-off of the fundamental guided mode is at 930 nm. For high pump powers (57 $\mu W/\mu m^2$), the spectral properties of the Anderson-localized modes are determined. The excitation power is then reduced to 0.57 $\mu W/\mu m^2$, cf. Fig. 2(c), which is close to the saturation power of a single quantum dot and time-resolved measurements are performed on the cavity emission spectrum. In such time-resolved measurements on the cavity peak, emission is recorded from all the quantum dots that are coupled to the cavity mode implying that the decay curves are generally multi-exponential. We concentrate here on the fastest component of the decay curves corresponding to emission from the quantum dot that couples best to the cavity. The measured decay curves (see Fig. 2(d) for representative examples) are fitted satisfactorily well with either single exponential, bi-exponential, or

#223550 - $15.00 USD Received 22 Sep 2014; revised 13 Nov 2014; accepted 14 Nov 2014; published 5 Dec 2014

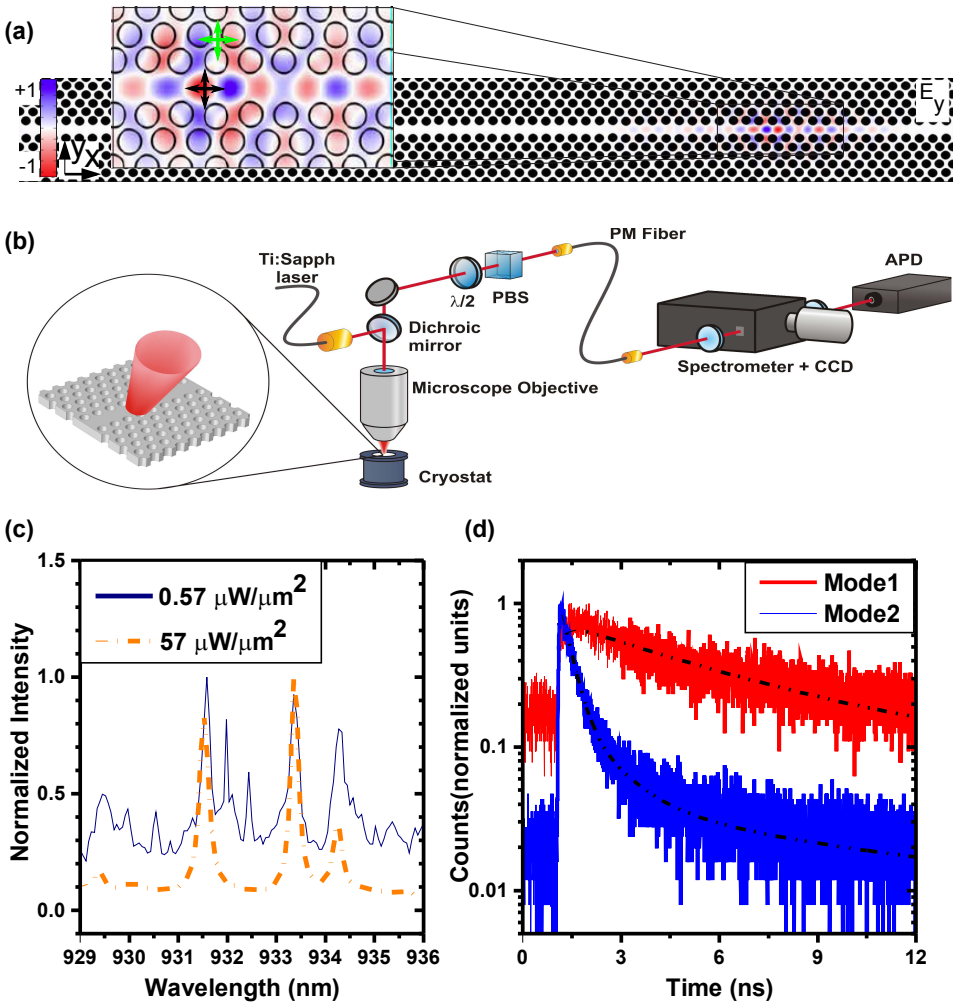


**Fig.** 2. **Samples and experimental method.** (a) Two-dimensional finite-element calculation of the $E_y$ component of an Anderson-localized mode along a PhCW with $\sigma = 1\%$ introduced disorder. The inset shows two dipoles placed at a node (green) and an antinode (blueblack) of the cavity, thus experiencing a very different local density of optical states. (b) Sketch of the experimental setup. See main text for detailed explanations. (c) Emission spectra of the sample under high excitation power (dashed curve) showing the Anderson-localized modes, and under low excitation power ( solid curve) showing Anderson-localized modes and quantum dot lines. (d) Examples of time-resolved photoluminescence decay curves of different Anderson-localized cavities fitted with multi exponentials (dashed lines). The pronounced differences in the decay times are attributed to the different spatial and spectral positioning of the dominant emitter feeding the cavities.

triple-exponential models after convolution with the 66 ps wide instrument response function of the setup acquired by sending the excitation laser reflected off the sample substrate through the setup. The same procedure is repeated for all of the observed Anderson-localized modes in the samples and very large variations are observed between different cavities. This procedure

#223550 - $15.00 USD Received 22 Sep 2014; revised 13 Nov 2014; accepted 14 Nov 2014; published 5 Dec 2014

enables us to acquire a large data set for the statistical analysis, which provides a lower bound on the actual Purcell enhancement that can be obtained in the system, since the detuning between the quantum dots and cavity modes is not controlled. In the second approach, the Purcell factor is probed directly by time-resolved photoluminescence experiments on a single quantum dot emission line after tuning it into resonance with an Anderson-localized cavity by varying the temperature from 10 K to 30 K [32]. The fast decay rate originates from recombination of the bright exciton of the resonant quantum dot. The Purcell factor is extracted by relating the measured decay rates to the average decay rate of 1.1 $ns^{-1}$ obtained from quantum dots in homogeneous environment. The optimum Purcell factor for a quantum dot perfectly matched spatially and spectrally to a cavity is given by $F_P = 3Q(\lambda/n)^3/4\pi^2V$, where n = 3.44 is the refractive index of the membrane and $Q$ and $V$ are the quality factor and mode volume of the cavity. From this relation a conservative upper bound on the mode volume of the Anderson-localized cavity can be extracted. It is worth mentioning that intrinsic non-radiative processes give rise to a small residual recombination rate in the quantum dots, which in the case of radiatively suppressed quantum dots leads to an underestimation of the inhibition factor [5]. For the enhanced quantum dots, on the contrary, the non-radiative decay rate is usually negligible.

## 3. Time-resolved measurements on Anderson-localized cavities

In the following we present the experimental data of the spontaneous emission dynamics recorded when collecting light from the Anderson-localized cavities. We study the two different waveguide branches and for different degrees of disorder. We observe a distribution of Purcell factors reflecting the statistical distribution of coupling coefficients due to the random nature of the Anderson-localized cavities and the spatial and spectral matching of the quantum dot emitters to the cavities. Figure 3 shows the statistics of the measured Purcell factor. The histogram in Fig. 3(a) shows the case of the secondary waveguide mode which can be probed with the quantum dots by choosing a sample with $a = 260$ nm and $r = 78$ nm, and in this case we focus on $\sigma = 0\%$ (i.e., only intrinsic disorder). We observe an average Purcell factor of 1.7 together with a variance of 0.5. We stress that the Purcell factor obtained from these types of measurements constitute lower bounds of the actual Purcell factor of a quantum dot tuned into resonance.

We also study the fundamental waveguide mode while varying $\sigma$ from 0% to 9%. For this purpose, a waveguide with parameters $a = 240$ nm and $r = 74$ nm is chosen, which has a bandedge at 932nm. The histograms in Figs. 3(b) to 3(d) include the experimentally extracted Purcell factor distributions for the waveguides with $\sigma = 0\%$, 3%, and 9%, respectively. The localized modes are found to span a spectral range between 3 nm and 7 nm. Compared to the measurements made at the high frequency waveguide mode, cf. Fig. 3(a), the Purcell factors are generally found to be considerably higher and have a broader distribution for the fundamental mode where also higher cavity Q-factors are observed, see insets of Figs. 3(a) to 3(d). The observed Purcell factors in this case range from 0.2 to 12, i.e., very pronounced suppression and enhancement is observed reflecting the broad range of coupling efficiencies found due to the statistical properties of the cavities. Figure 3(e) shows the mean and variance of the Purcell factor for waveguides with different amounts of disorder. The mean value of Purcell factor for individual distribution varies between 3.5 to 5.8 depending on the degree of disorder. There is also a clear trend in the mean value of Purcell factors versus extrinsic disorder. Increasing intentional disorder up to 3% tends to increase the mean value of the Purcell factor from 3.5 to 5.5 while further increase in the disorder amount decreases the mean value of the Purcell factor. The collected statistics reveal that there is a significant enhancement of light-matter interaction in the disordered medium.

We note that the uncertainty on each individual Purcell factor, due to the uncertainty in

#223550 - $15.00 USD Received 22 Sep 2014; revised 13 Nov 2014; accepted 14 Nov 2014; published 5 Dec 2014

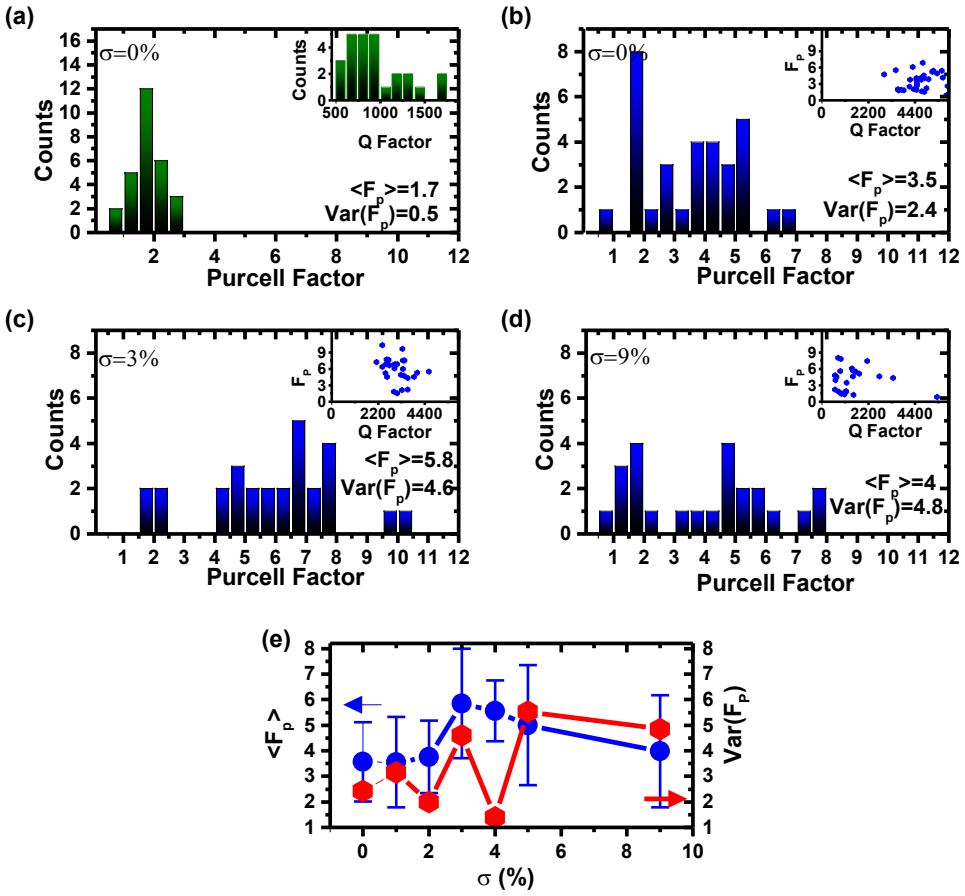


**Fig.** 3. **Statistics of decay rates measured on the Anderson-localized cavities** (a) Histogram of the measured decay rates from Anderson-localized modes appearing along an unperturbed PhCW ($\sigma = 0\%$) with a = 260 nm and r = 78 nm for the high-energy guided mode. The inset shows the histogram of the cavity Q-factors. (b),(c) and (d) Histograms displaying the Purcell factor measured on Anderson-localized modes for the fundamental guided mode of a PhCW with a = 240 nm and r = 74 nm and for $\sigma = 0\%$, $\sigma = 3\%$ $\sigma = 9\%$, respectively. The insets show the measured Purcell factor vs. the corresponding cavity Q-factor. The lack of clear correlation between Q factor and decay rates is attributed to the uncontrolled spatial and spectral matching of the dominant emitter to the cavity. (e) Mean and variance of the measured Purcell factors vs. disorder degree for the data of (b)-(d). The variance is defined as $\mathrm{Var}(F_p) = \langle F_p^2 \rangle - \langle F_p \rangle^2$ and the error bars in $\langle F_p \rangle$ are the square root of the variance.

the fitting routine of the decay rate, is in the range of $\Delta F_p \approx 0.4$. This value is smaller than the square root of the variance of the Purcell factor reported in Fig. 3(e). The variance of the Purcell factor distributions shown in Fig. 3(e) is due to the inherent statistical distribution of the Anderson-localized cavities including the random positioning of the individual QDs with respect to the cavities. While the former is determined by the amount of disorder in the structure [30], the latter is independent of disorder. The interplay between these two mechanisms gives rise to the non-trivial dependence of the variance of the Purcell factor with disorder in Fig. 3(e).

#223550 - $15.00 USD Received 22 Sep 2014; revised 13 Nov 2014; accepted 14 Nov 2014; published 5 Dec 2014

## 4. Time-resolved measurements on single quantum dots

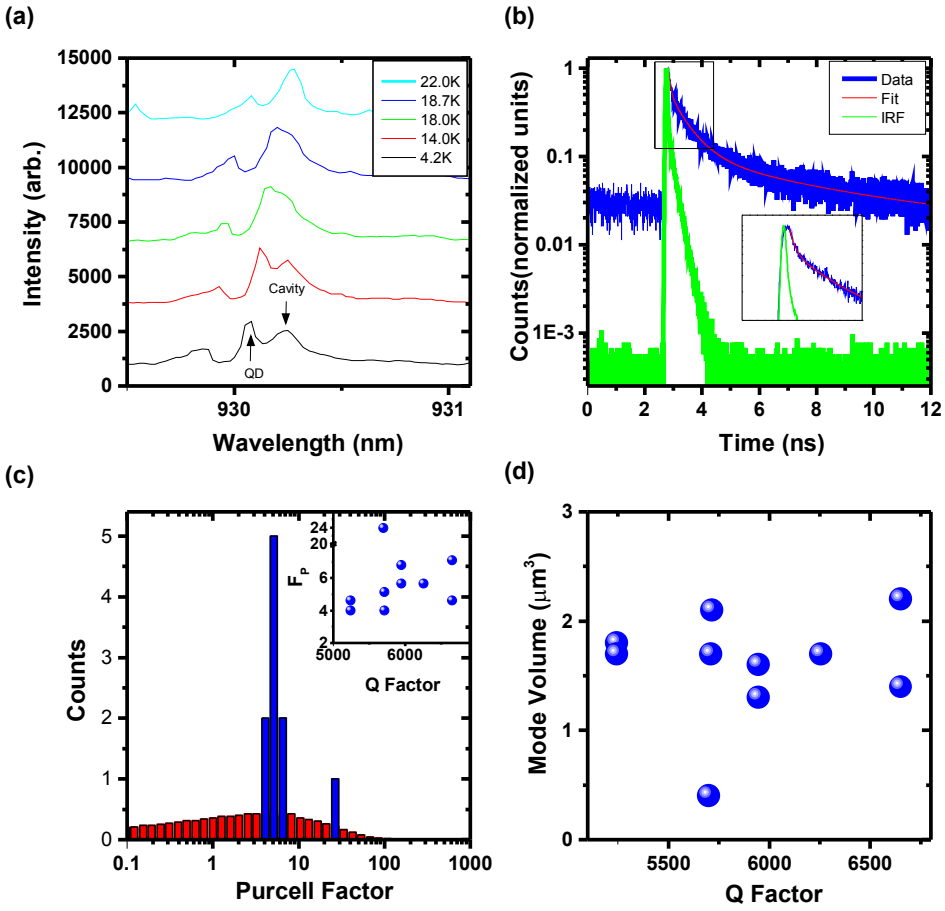


**Fig.** 4. **Statistical distribution of Purcell factors from single quantum dots on resonance with Anderson-localized cavities.** (a) Emission spectrum of the fastest quantum dot (Purcell factor of 23.8±1.5) while temperature tuning it through resonance of an Anderson-localized mode. (b) Decay curve recorded from the quantum dot in (a) at resonance with the cavity. The fit is shown as the solid red line. The green curve is the instrument response function(IRF) of the detector). (c) Purcell factor statistics obtained after tuning single quantum dots into resonance for a PhCW with r = 69 nm, a = 230 nm, and $\sigma = 1\%$ (Blue histogram). The red histogram shows the theoretically calculated distribution using the theory in [29]. (d) Extracted upper bound on the mode volume vs. the corresponding cavity Q-factor.

In the previous section, we found a maximum in the average Purcell factor for quantum dots coupled to Anderson-localized cavities appearing near the cutoff of the fundamental guided mode. In order to measure the Purcell factor more precisely, the detuning between quantum dot and cavity is controlled through temperature and the decay rate is extracted on resonance. Figure 4(a) shows the spectrum of a single quantum dot while temperature tuning it across the resonance of an Anderson-localized cavity. We have repeated this procedure for a total of 10 different quantum dots along the PhCW. The statistics are plotted in Fig. 4(c), where we observe

#223550 - $15.00 USD Received 22 Sep 2014; revised 13 Nov 2014; accepted 14 Nov 2014; published 5 Dec 2014

Purcell factors in the range of 4 - 7 together with a quantum dot with a Purcell factor as high as 23.8. For comparison, the theoretically predicted distributions are also plotted in Fig. 4(c). The theory predicts a wide range of Purcell factors but the experiment has focused on extracting the large-value tail of the distribution due to the limited statistics available in the experiment. The inset in Fig. 4(c) plots the measured Purcell factors vs. the cavity Q, and no clear correlation is observed, which is attributed to the fact that the quantum dots are positioned randomly relative to the electric field of the localized cavities. Using the theoretical expression for the Purcell factor, we can estimate upper bounds on the mode volume of the individual Anderson-localized modes that are plotted in Fig. 4(d). The extracted values range between 0.5 to 2.2 $\mu$m$^3$, where we stress that spatial mismatch mentioned above will imply that these values are significantly overestimated, and likely to be consistent with the mode volumes in the range of 0.07 - 0.1 $\mu$m$^3$ recently obtained from random lasing experiments [28].

Finally we analyze in detail the case of a Purcell factor of 23.8$\pm$1.5, shown in Fig. 4(b). In this case the upper bound for the mode volume is 0.40$\pm$0.03 $\mu m^3$ and the spatial positioning and dipole orientation is likely to be close to optimal. The criterion for strong coupling between a quantum dot and a cavity is $g/\kappa > 1/4$, where $\kappa = 2\pi c/\lambda Q$ is the loss rate of the cavity, $g$ is the coupling strength between the emitter and the cavity, $c$ is speed of light in vacuum, and $\lambda$ is the wavelength of emitted photon. For this particularly fast quantum dot this ratio is $g/\kappa = 0.130 \pm 0.004$, which indicates that the cavity is in the weak-coupling regime, but close to the onset of strong coupling. Another important figure-of-merit is the $\beta$-factor that specifies the fraction of recombination events of the quantum dot that leads to a photon in the cavity. An estimate of $\beta$ is obtained by comparing the decay rate of the quantum dot when tuned away from resonance to the rate on resonance [8]. We obtained $\beta = 86\%$ for the highly enhanced quantum dot. This number is limited by the applied tuning range of the quantum dot in this experiment. From measurements on other quantum dots that are suppressed and therefore not well coupled to cavity modes we estimate that a typical rate for coupling to other channels than the cavity would be 0.15 ns$^{-1}$. From such an estimate we conclude that the quantum dots are coupled to the Anderson-localized cavities with $\beta$-factors reaching as high as 99%.

## 5. Conclusions

In conclusion, we have presented a statistical analysis of the emission dynamics from single quantum dots embedded in disordered PhCWs. The measurement of the decay dynamics from Anderson-localized modes enables efficient collection of a large amount of data. These measurements provide detailed insight about the statistical properties of QED in disordered PhCWs. We observe a dependence of the distribution of the Purcell factor with the amount of disorder. We attribute this dependence to the interplay between the statistical distribution of the Anderson-localized modes and the random positioning of the individual QDs with respect to them. Measuring the decay rate of single quantum dots that are spectrally tuned across the cavities allows to reliably extract the Purcell factor. Hence, we observed Purcell factors in the range of 4-7 together with an extraordinarily large Purcell factor of 23.8$\pm$1.5. The experimental data are compared to theory where a very broad distribution of Purcell factors is expected that cannot be fully resolved in the present experiment. This work demonstrates the promising potential of disordered nanophotonic structures for QED experiments and shows that the transition to the strong-coupling regime should be within experimental reach [33].

## Acknowledgments

We gratefully acknowledge financial support from the Danish council for independent research (natural sciences and technology and production sciences), and the European research council (ERC consolidator grant “ALLQUANTUM”).

#223550 - $15.00 USD Received 22 Sep 2014; revised 13 Nov 2014; accepted 14 Nov 2014; published 5 Dec 2014